Check for updates

View Article Online
View Journal

NJC

Accepted Manuscript

This article can be cited before page numbers have been issued, to do this please use: T. C. D. A. Lage, T. M. S. Maciel, Y. C.C. Mota, F. Sisto, J. R. Sabino, J. Carinhanha, I. Figueiredo, C. Masia, A. de Fatima, S. A. Fernandes and L. V. Modolo, *New J. Chem.*, 2018, DOI: 10.1039/C8NJ00072G.

This is an Accepted Manuscript, which has been through the Royal Society of Chemistry peer review process and has been accepted for publication.

Accepted Manuscripts are published online shortly after acceptance, before technical editing, formatting and proof reading. Using this free service, authors can make their results available to the community, in citable form, before we publish the edited article. We will replace this Accepted Manuscript with the edited and formatted Advance Article as soon as it is available.

You can find more information about Accepted Manuscripts in the author guidelines.

Please note that technical editing may introduce minor changes to the text and/or graphics, which may alter content. The journal's standard Terms & Conditions and the ethical guidelines, outlined in our author and reviewer resource centre, still apply. In no event shall the Royal Society of Chemistry be held responsible for any errors or omissions in this Accepted Manuscript or any consequences arising from the use of any information it contains.

Please do not adjust margins

View Article Online
DOI: 10.1039/C8NJ00072G

ARTICLE

In vitro inhibition of *Helicobacter pylori* and interaction studies of lichen natural products with jack bean urease

Received 00th January 20xx,
Accepted 00th January 20xx

DOI: 10.1039/x0xx00000x

www.rsc.org/

Tiago C. A. Lage,[a] Thamilla Maria S. Maciel,[b] Yane C. C. Mota,[c] Francesca Sisto,[d] José R. Sabino,[e] Josué C. C. Santos,[b] Isis M. Figueiredo,[b] Carla Masia,[d] Ângelo de Fátima,[f,*] Sergio A. Fernandes,[a,*] Luzia V. Modolo[c]

The interaction of (*S*)-(-)-usnic acid (**2**) and fumarprotocetraric acid (**3**), isolated from *Cladonia rappii* (lichen), and commercial (*R*)-(+)-usnic acid (**1**) with urease was investigated *in vitro* by molecular spectroscopy at pH 7.4 and kinetics experiments using jack bean type III urease. All lichen compounds tested interact with urease by statistic quenching mechanism forming non-fluorescent complexes that change the native protein structure. Complexes formation were spontaneous and stabilized mainly by electrostatic forces, in which interaction magnitude was determined to be **3** < **2** < **1**. Compound **2**, whose tridimensional structure is here disclosed, acts as mixed inhibitor while compounds **1** and **3** function as competitive ones. The (R)-(+)-UA (**1**) were the most efficient lichen metabolite with respect to impairment of the growth of five *H. pylori* strains. The minimum inhibitory concentrations (MIC) for the lichen metabolites tested were lower (from 2- to 7.8-fold) than those of omeprazole (reference drug) against all *H. pylori* strains tested. Overall, the lichen metabolites **1**-**3** are promising lead compounds for the design of more efficient urease inhibitors for the treatment of *H. pylori* infections.

Introduction

Lichens are symbiotic organisms formed by green algae or cyanobacterium (photobiont portion) and a fungal partner (mycobiont). Such relationship is quite complex and provides with a fantastic pool of secondary metabolites, mostly due to the fungal component.[1] The natural compounds produced by lichens have been shown to be valuable for medicinal purposes.[2] Usnic acid (**UA**; Figure 1), discovered in 1843, is the most studied lichen metabolite[3] likely due to the fact that both enantiomeric forms are unique to lichens and particularly abundant in *Alectoria*, *Cladonia*, *Usnea*, *Lecanora*, *Ramalina* and *Evernia* species.[4] The **UA** exhibits a broad variety of biological properties, which include antimicrobial,[5] antioxidant,[6] antiviral,[7] antiproliferative/cytotoxic,[7,8] anti-inflammatory[9] and wound healing[10] activities.

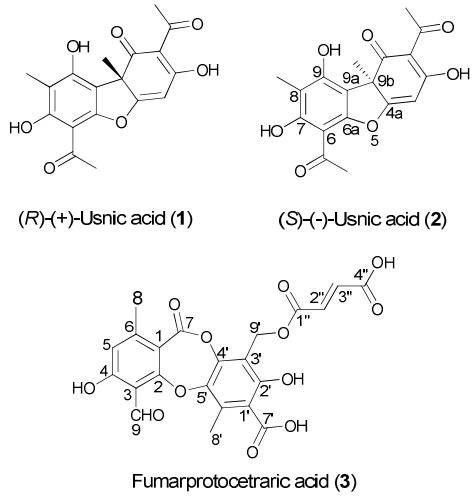

Figure 1. Secondary metabolites produced by lichens.

[a] *Grupo de Química Supramolecular e Biomimética (GQSB), Departamento de Química, Universidade Federal de Viçosa, Viçosa, MG, 36570-900, Brazil. E-mail: sefernandes@gmail.com.*
[b] *Laboratório de Instrumentação e Desenvolvimento em Química Analítica (LINQA), Instituto de Química e Biotecnologia, Universidade Federal de Alagoas, Maceió, AL, 57072-900, Brazil.*
[c] *Grupo de Estudos em Bioquímica de Plantas (GEBioPlan), Departamento de Botânica, Universidade Federal de Minas Gerais, Belo Horizonte, MG, 31270-901, Brazil.*
[d] *Department of Biomedical, Surgery and Dental Sciences, Università degli Studi di Milano, Milano, Italy.*
[e] *Grupo de Cristalografia, Instituto de Física, Universidade Federal de Goiás, Goiânia, GO, 74690-900, Brazil.*
[f] *Grupo de Estudos em Química Orgânica e Biológica (GEQOB), Departamento de Química, Universidade Federal de Minas Gerais, Belo Horizonte, MG, 31270-901, Brazil. E-mail: adefatima@qui.ufmg.br*

The structural result for (**1**) was deposited with the Cambridge Crystallographic Data Centre as Supporting Information, CCDC number: 1033509. Copies of the data can be obtained free of charge upon application to CCDC, 12 Union Road, Cambridge CB2 1EZ, United Kingdom (Fax: (44) 1223 336-033 or by the e-mail: deposit@ccdc.cam.ac.uk).

Electronic Supplementary Information (ESI) available: [details of any supplementary information available should be included here]. See DOI: 10.1039/x0xx00000x

Published on 13 February 2018. Downloaded by Fudan University on 14/02/2018 15:52:19.

New Journal of Chemistry Accepted Manuscript

Please do not adjust margins

View Article Online
DOI: 10.1039/C8NJ00072G

Published on 13 February 2018. Downloaded by Fudan University on 14/02/2018 15:52:19.

Fumarprotocetraric acid (**FPA**; **3**) is a depsidone derivative first isolated in 1904 from the lichen *Cetraria islandica*.[11] This class of compounds was shown to inhibit the HIV-1 integrase activity[12] and lipid peroxidation, besides functioning as expectorant[13] and herbicide.[14] Substances able to inhibit the activity of *Helicobacter pylori* urease have been used for the treatment of diseases associated with infections caused by this gram-negative bacterium. The mechanism by which *H. pylori* colonizes the stomach involves the production of urease and its release to the medium to increase the pH around bacterial microenvironment *via* conversion of urea to ammonia.[15] In addition, it is reported that ammonia can also contribute to the gastric lesions.[16] Then, the development of new urease inhibitors has been an interesting approach for the treatment of *H. pylori*-associated diseases.

This work focused on investigation of the potential of the lichen secondary metabolites (*R*)-(+)-usnic acid (**1**), (*S*)-(-)-usnic acid (**2**) and fumarprotocetraric acid (**3**) to inhibit, *in vitro*, urease activity and *H. pylori* growth. Kinetics studies were performed to reveal the mechanism by which these natural products inhibit the enzyme. The urease-inhibitor interactions were extensively explored by molecular fluorescence assays. The X-ray structure of compound **2**, herein isolated from the lichen *Cladonia rappii*, is also disclosed.

Results and discussion

Structure elucidation

The (*S*)-(-)-usnic acid [(*S*)-(-)-**UA** (**2**)] was successfully isolated from *C. rappii* as yellow needles whose molecular formula ($C_{18}H_{16}O_7$) was determined on the basis of HRESITOFMS analysis (*m/z* 343.0792, for $C_{18}H_{15}O_7$, $[M\text{-}H]^-$). The melting point obtained for compound **2** was 193.7-194.3 °C (Lit.: 200-201 °C).[17] Signal correspondent to the conjugated cyclic ketone group was observed at 1688 cm^{-1} in the infrared spectrum. The ketone groups were noted at 1627 cm^{-1} and 1605 cm^{-1}. The antisymmetric and symmetric ν(COC) signals for aryl alkyl ethers were assigned at 1283 and 1067 cm^{-1}, respectively.[18] The signal at 3400 cm^{-1}, typical of –OH groups absorption, was absent in the IR spectrum due to the formation of an intra-molecular hydrogen-bonding, confirmed by X-ray analysis (Figure 2).

The ^{1}H NMR spectra for compound **2** exhibited singlet signals only. The most characteristic signal was recorded at δ_H 18.84 for the 3-OH hydrogen, with the two other signals at δ_H 13.30 (7-OH) and δ_H 11.02 (9-OH). The signals correspondent to carbon atoms bonded to –OH groups were recorded, respectively, at δ_C 191.6, 163.8 and 157.4 in the ^{13}C NMR spectrum. All the spectral data are in agreement with those reported elsewhere.[18,19] The stereochemistry at C-9b was determined to be as (*S*)-(-) configuration based on the negative sign of rotation ($[\alpha]_{20}^{d}$ = -391) for the isolated usnic acid (**2**). This value presents an opposite sign when compared with the reported data for the isomer [(*R*)-(-)-**UA** (**1**)].[4,5a]

The compound **2** chirality was also confirmed by X-ray Crystallography analysis (Figure 2). The experimental setup using Cu-Kα was successful due to the oxygen atoms anomalous scattering. In this case, the anomalous signal of an oxygen atom is about 5% that of the scattering power of a point electron, but the unit cell contains 56 O atoms, because there are two independent molecules of 2 in the asymmetric unit related by a non-crystallographic 2-fold axis. As a result, the anomalous signal of the whole unit cell is comparable to the scattering of about 2.8 electrons. The chirality was determined with respect to the Flack parameter of 0.026(18), calculated using 2266 intensity quotients.[20] Besides, an interesting feature is the occurrence of a short intramolecular hydrogen bond involving the atoms O14-H…O16, with donor-acceptor distance of 2.402(2) and 2.403(2) Å, in the molecules A and B, respectively. The hydrogen atoms were located and freely refined close to the midway. Therefore, the C4–O14 and C15–O16 bond distances are in the range from 1.268(2) Å to 1.286(2) Å.

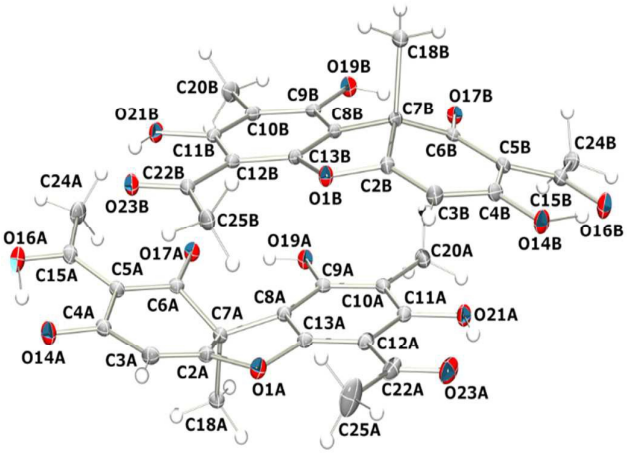

Figure 2. Ortep representation of (*S*)-(-)-usnic acid (**2**) asymmetric unit. Atomic ellipsoids are drawn at 30% of probability level.

The fumarprotocetraric acid [**FPA**; (**3**)] was precipitated as an amorphous powder of molecular formula equal to $C_{22}H_{16}O_{12}$ as attested by HRESITOFMS (*m/z* 471.0603, for $C_{22}H_{15}O_{12}$, $[M\text{-}H]^-$). The spectral data are in agreement with those described in the literature.[18,21] Antisymmetric and symmetric ν(C=C) stretching signals were assigned at 3094 cm^{-1} of IR spectrum. The ν(C=O) for phenyl-ester group was at 1747 cm^{-1}. The ν(C=O) frequency for the other carbonyl groups in compound **3** was found to be quite lower than the expected due to a conjugation of carbonyl groups and hydrogen-bonding. Thus, a band for methyl-ester and chain carboxylic acid was observed at 1699 cm^{-1} and at 1655 cm^{-1} for aldehyde and phenyl carboxylic acid. Bands for ν(C=C) were registered at 1615 cm^{-1} and at 1575 cm^{-1} for ν(C=C) of aromatics.[18] Similarly to the observed for compound 2, ^{1}H NMR spectrum exhibited only singlets, indicating the presence of two methyl groups singlets at δ_H 2.42 and 2.45. The methylene (H-9') signal appeared at δ_H 5.30 and δ_H 6.84 for aromatic hydrogen. The signals for double bond hydrogens at 2" and 3" were superimposed as a singlet due to the same chemical environment at δ_H 6.64. However, the reaction of

New Journal of Chemistry Accepted Manuscript

This journal is © The Royal Society of Chemistry 20xx
Please do not adjust margins

Please do not adjust margins
View Article Online
DOI: 10.1039/C8NJ00072G

Published on 13 February 2018. Downloaded by Fudan University on 14/02/2018 15:52:19.

FPA (3) with triethylamine produced a salt (3a) (Figure S1; Supporting information) that yielded multiplicity of double bound signals at δ_H 6.67, J = 15.6 Hz and δ_H 6.28, J = 15.6 Hz, respectively. The J value indicated that these signals correspond to *trans* double bond. The signal for aldehyde hydrogen was observed at δ_H 10.57. A singlet at δ_H 11.97 corresponds to the 2'-OH group, whose signal appears in a downfield region due to a hydrogen-bond and a conjugation with a carboxylic acid. In addition, ^{13}C NMR spectrum showed 22 signals: two for methyl carbons (δc 14.6 and 21.3), one for methylene group (δc 56.8), twelve for two aromatic rings, ranging from δc 112.0 to δc 163.9 and two for *trans* double bond carbons (δc 132.1 and 135.0). The signal for the aldehyde carbon occurs in δc 191.6 and carbonyl carbons were confirmed by signals at δc 170.1 and 165.6, for carboxylic acids, δc 160.9 for cyclic ester and δc 164.6 for chain ester. The set of ^1H and ^{13}C NMR spectra (Figures S2-S6) of compounds 2 and 3 are in the supporting information.

Effect of lichen secondary metabolites on urease activity

Purified type III urease from *Canavalia ensiformis* (jack bean) was used to evaluate the ability of lichen metabolites to inhibit the ureolytic activity of this hydrolase. The **FPA** (**3**) was found to be as efficient as hydroxyurea (HU; inhibitor-reference) as it inhibited urease activity by 63.7% when used at 1 mM (Figure 3a). At the same experimental conditions, (*R*)-(+)-**UA** (**1**) and (*S*)-(-)-**UA** (**2**) inhibited the ureolytic activity by 45.3 and 33.1%, respectively. Kinetics assays were further performed to determine the mechanism by which the lichens metabolites inhibit urease activity. The double-reciprocal plots indicate that (*R*)-(+)-**UA** (**1**) and **FPA** (**3**) are typical competitive inhibitors as urea K_M increased and urease V_{max} was unaffected by the presence of these compounds regardless of the inhibitor concentration tested (Figures 3b and 3d). On the other hand, (*S*)-(+)-**UA** (**2**) works as a mixed inhibitor, in which both K_M and V_{max} were affected in reactions containing increasing concentration of inhibitor (Figure 3c). Also, the lines in the double reciprocal plot intersect one another in the second quadrant (Figure 3c). Other natural products such as protocatechuic aldehyde, syringaldehyde and vanillin were shown to be mixed inhibitors towards urease[22]. Competitive inhibitors compete with the substrate for the enzyme active site and are related to the formation of EI (enzyme-inhibitor) complexes whose equilibrium dissociation constant (or inhibitor constant) is defined as K_i. Mixed-type inhibitors are capable to bind to both the free enzyme, generating EI complex, and the enzyme-substrate (ES) complex (providing ESI complex), therefore being associated to the additional equilibrium dissociation constant K'_i. The lower the K_i or K'_i is, the higher the inhibitor's affinity for the enzyme active and allosteric(s) sites, respectively.[23] The affinity of compounds **1** and **3** for urease active site was determined to be similar and 3.1-fold higher than that of compound **2** (Table 1). As for the mixed inhibitor (*S*)-(+)-**UA** (**2**), its affinity for allosteric site(s) was found to be 2.5-fold lower when compared to that for urease active site (Table 1).

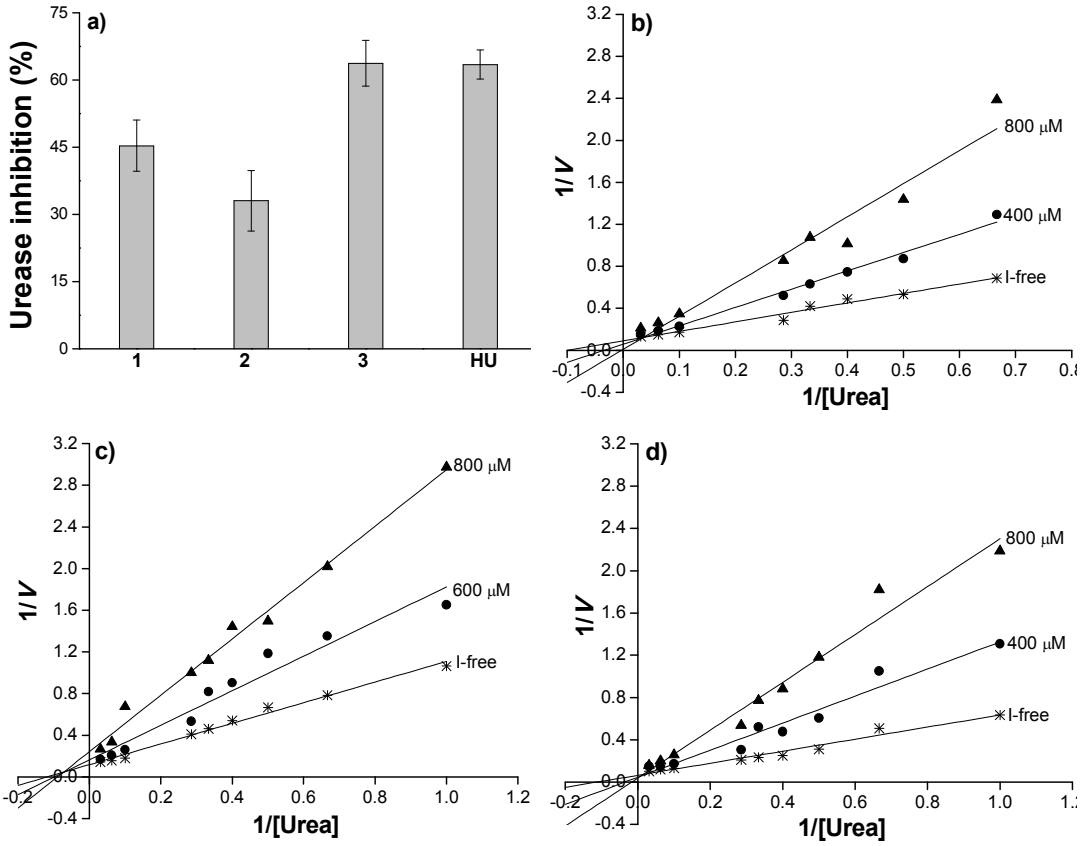

Figure 3. Effect of lichen metabolites on the activity of jack bean urease. For the screening assay (a), enzyme activity was assessed from reactions containing 1 mM compound-test, 10 mM urea and jack bean type III urease (12.5 mU). As for the kinetics assay, increasing concentrations of urea were incubated for

New Journal of Chemistry Accepted Manuscript

Please do not adjust margins

View Article Online
DOI: 10.1039/C8NJ00072G

10 min with urease in the absence of inhibitor (I-free) or presence of (*R*)-(+)-**UA** (**1**) (b), (*S*)-(-)-**UA** (**2**) (c) or **FPA** (**3**) (d) at indicated concentrations. When applicable, hydroxyurea (HU) was used as reference of urease inhibitor.

Table 1. Effect of lichens secondary metabolites on jack bean urease kinetics. Urea (1 to 32 mM) was incubated for 5 min with jack bean type III urease in the absence or presence of compounds tested at 0.2, 0.4 or 0.8 mM. The K_M and V_{max} values averaged 7.3 ± 1.2 mM and 10.0 ± 0.6 μmol NH_4^+ min^{-1} mg^{-1} urease, respectively.

Urease inhibitor	K_i (mM)	K'_i (mM)
(*R*)-(+)-**UA** (**1**)	0.36 ± 0.11	N/A
(*S*)-(-)-**UA** (**2**)	1.10 ± 0.54	2.94 ± 1.71
FPA (**3**)	0.34 ± 0.05	N/A

K_i refers to as the equilibrium dissociation constant for urease-inhibitor (EI) complex and K'_i corresponds to the equilibrium dissociation constant for urease-urea-inhibitor (ESI) complex. Values are the mean ± standard error. N/A, not applicable.

Interaction between lichen secondary metabolites and jack bean urease

The interaction studies between compounds **1-3** and urease were carried out to explore the mechanism of enzyme inhibition exhibited by the lichen natural products. Proteins that usually present tryptophan (Trp), tyrosine (Tyr) and phenylalanine (Phe) residues have intrinsic fluorescence. The Phe residues exhibit low fluorescence quantum yield, while that of Tyr ones is almost completely quenched by carboxyl groups, disulfide bonds or Trp.[24] Urease from *Canavalia ensiformis* (jack bean) contains four Trp residues at positions 495, 648, 708, and 728.[25] The urease intrinsic fluorescence is roughly a result of Trp residues contribution, which then can be used as intrinsic fluorophores for studies of protein-ligand interactions and ligand-induced conformational changes around binding site.[26]

The interaction between urease and lichen compounds **1-3** was assessed by stationary fluorescence spectroscopy based on quenching effect. The variation of urease fluorescence intensity upon addition of (*R*)-(+)-**UA** (**1**) (a competitive inhibitor) is shown in Figure 4a. The Trp residue is known to have high sensitivity to the microenvironment polarity.[24] The maximum emission observed at 334 nm for the native urease indicates that Trp residues are partly protected from the solvent.[27] The blue shift of urease fluorescence maximum emission from 334 to 332 nm could be related to conformational changes induced by the interaction of (*R*)-(+)-**UA** (**1**) with urease (Figure 4a). This indicated that a decrease of microenvironment polarity around Trp residues took place.[24,27] Similar results were observed for (*S*)-(-)-**UA** (**2**) associated in which the blue shift was from 334 to 333 nm. Fumarprotocetraric acid (**3**), however, presented red shift from 334 to 335 nm due to increase of microenvironment polarity around Trp residues.

The Stern-Volmer equation was then used to examine the mechanism of interaction between lichen compounds **1-3** and urease:

$$\frac{F_0}{F} = 1 + K_{SV}[Q] \qquad \text{equation (1)}$$

where, F_0 and F are the fluorescence intensities in absence and presence of the ligands, respectively; [Q] is the ligand (quencher) concentration and K_{SV} is the Stern-Volmer quenching constant.[29,30] The binding constant (K_b) was calculated according to equation 2:

$$\log\left[\frac{F_0 - F}{F}\right] = \log K_b + n\log[Q] \qquad \text{equation (2)}$$

K_b is the binding constant, *n* is the number of binding sites. The equations (1) and (2) were then linearized to obtain the plots of Figures 4b and 4c, respectively, to determine K_{SV}, K_b and *n* values.[30]

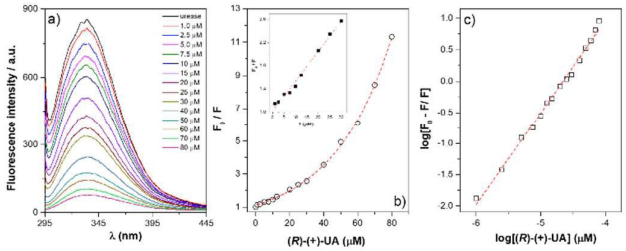

Figure 4. Urease (1.0 μM) emission spectral profile in the presence of different concentrations of (*R*)-(+)-**UA** (**1**) at pH 7.4 and 30 °C (a). Stern-Volmer quenching plot (b). The inset corresponds to microenvironment polarity around Trp residues the linear plot. Double logarithmic curve for binding constant calculation (c).

The temperature effect on the interaction between lichen compounds **1-3** and urease was further investigated and the results summarized in Table 2. The exponential profile of K_{SV} plot (Figure 4b) indicates that either all Trp residues are accessible to the quencher or one of Trp residues is solely responsible for light emission.[27] The concentration liner range obtained when using lichen compounds from 1.0 to 30 μM was employed to calculate K_{SV} values (Table 2) and determine mechanism of preferential quenching. The K_{SV} values decreased upon increment of temperature, indicating the occurrence of static quenching, as higher temperatures affect the protein-ligand complex stability[31] (Table 2). On the other hand, increment in K_{SV} values accompanied of increasing in temperature would lead to typical dynamic quenching due to larger diffusion coefficient values.

The ligand affinity toward urease is a relevant parameter for protein-ligand interaction studies and thereby helps to understand the mechanism by which compounds **1-3** inhibit urease activity. The binding constant (K_b) expresses the strength of interaction between a ligand and a due protein and for the case of lichen metabolites it was found that the interaction between (*R*)-(+)-**UA** (**1**) and urease was stronger than that of (*S*)-(-)-**UA** (**2**) and **FPA** (**3**) (Table 2). The K_b values for lichen compounds **1-3** toward urease were in the same

Published on 13 February 2018. Downloaded by Fudan University on 14/02/2018 15:52:19.
New Journal of Chemistry Accepted Manuscript

This journal is © The Royal Society of Chemistry 20xx
Please do not adjust margins

View Article Online
DOI: 10.1039/C8NJ00072G

range of those reported for the interaction between pentachlorophenol (3.85×10^3 M^{-1} at 32 °C),[26] $K_2Cr_2O_7$ (1.96×10^4 M^{-1} at 29 °C)[31] and Cu(II) (3.89×10^5 M^{-1} at 37 °C for [Cu(II)] < 16 μM)[32] and jack bean urease. However, these authors did not evaluate the potential of pentachlorophenol, $K_2Cr_2O_7$ and Cu(II) as urease inhibitors.

Indeed, (*R*)-(+)-**UA** (**1**) interacted more effectively with urease likely due to this ability to fit well into urease active site. This result is supported by kinetics one in which (*R*)-(+)-**UA** (**1**) was determined to be a competitive inhibitor (Figure 3; Table 1). Urease was found to be enantioselective for usnic acid isomers as the K_b values for (*R*)-(+)-**UA** (**1**) were greater than those for (*S*)-(-)-**UA**. Other enantioselective proteins are described in the literature. For instance, human serum albumin (HSA) was shown be enantioselective to (*R*)-ibuprofen (anti-inflammatory agent)[33] and (*S*)-diclofop-methyl (pesticide).[34] Therefore, K_b value allows establishing whether a protein is enantioselective to a certain isomer. Additionally, the K_i values obtained from kinetics assay at 25 °C revealed that the affinity of (*R*)-(+)-**UA** (**1**) to urease active site is 3-fold higher than that of (*S*)-(+)-**UA** (**1**) (Table 1). Similar results were obtained for K_b whose value at 23 °C for the former was 2.9-fold greater than that for the latter (Table 2).

Similarly, to the observed for K_{SV} values, the binding constants (K_b) for lichen compounds **1-3** toward urease decreased with increment of temperature, confirming the occurrence of static quenching. According to equation 2, *n* corresponds to the number of occupied sites by the ligand in the urease structure. The *n* values varied from 0.92 to 1.42, indicating that the interactions among these ligands and urease occurs in the ratio of 1:1.

Thermodynamic parameters (ΔH and ΔS) were then obtained using the linearized Van't Hoff equation (equation 3) from interaction assays performed at different temperatures.[35] These parameters permit to deduce the type of forces involved in urease-inhibitor interaction (Table 2). The Gibbs free energy (ΔG) was calculated according to equation 4.

$$\ln K_b = -\frac{\Delta H}{R}\cdot\left[\frac{1}{T}\right] + \frac{\Delta S}{R} \qquad \text{equation (3)}$$

$$\Delta G = \Delta H - T\Delta S \qquad \text{equation (4)}$$

where T is the temperature in Kelvin (K) and R is the ideal gas constant (8.314462 J K^{-1} mol^{-1}). The Figure S7 (Supporting information) shows a graphical representation of linearized Van't Hoff equation (supporting information).

Table 2. Binding and thermodynamics parameters for urease interaction with lichen compounds **1**-**3**.

Lichen compound	T (°C)	Binding parameters					Thermodynamic parameters		
		K_{SV} (10^4 M^{-1})	r	K_b (10^5 M^{-1})	*n*	r	ΔG (kJ mol^{-1})	ΔH (kJ mol^{-1})	ΔS (J mol^{-1})
(*R*)-(+)-**UA** (**1**)	23	5.25 ± 0.18	0.9948	52.5 ± 3.7	1.41 ± 0.07	0.9898	-65.70		
	30	5.05 ± 0.16	0.9955	35.5 ± 4.9	1.42 ± 0.06	0.9823	-65.96	-54.81	+36.73
	38	4.60 ± 0.17	0.9936	18.6 ± 2.4	1.32 ± 0.07	0.9862	-66.23		
(*S*)-(-)-**UA** (**2**)	23	5.48 ± 0.30	0.9870	18.3 ± 4.2	1.30 ± 0.09	0.9836	-35.58		
	30	4.86 ± 0.28	0.9848	15.7 ± 4.5	1.29 ± 0.08	0.9804	-35.92	-21.02	+ 49.10
	38	5.00 ± 0.28	0.9859	12.3 ± 4.4	1.27 ± 0.07	0.9795	-36.30		
FPA (**3**)	23	3.29 ± 0.18	0.9861	0.28 ± 0.01	0.96 ± 0.02	0.9955	-25.24		
	30	3.52 ± 0.19	0.9871	0.25 ± 0.01	0.95 ± 0.01	0.9979	-25.50	-14.28	+ 36.98
	38	3.81 ± 0.23	0.9830	0.21 ± 0.01	0.92 ± 0.02	0.9978	-25.78		

The negative values obtained for ΔG indicate that the interaction between lichen compounds **1-3** and urease is thermodynamically spontaneous. The possible scenarios for the relationship amongst the main forces involved in urease-inhibitor interaction and enthalpy and entropy include ΔH > 0 and ΔS > 0 (hydrophobic forces); ΔH < 0 and ΔS > 0 (electrostatic forces) and ΔH < 0 and ΔS < 0 (hydrogen bonding and Van der Waals forces).[36] As for the lichen metabolites tested, ΔH values were negative, while ΔS ones were positive indicating exothermic process and the interaction occurred through electrostatic forces. Hence, once urease-inhibitor interaction was established, the protein-associated water molecules are displaced by the ligand, a condition that was responsible for a positive change in entropy system during the interaction.

The three-dimensional fluorescence spectrum allows obtaining more detailed information about typical conformational changes in the secondary structure of a protein.[30] The three-dimensional fluorescence spectra for urease by itself or complexed with (*R*)-(+)-**UA** (**1**) are presented in Figure 5. Three-dimensional fluorescence graphics of free urease and urease-(*R*)-(+)-**UA** (**1**) complex show peak 1, which corresponds to Rayleigh scattering, characterized by radiation re-emission ($\lambda_{ex} = \lambda_{em}$) from water (solvent) (Figure 5). Thereby a small fraction of the absorbed radiation is scattered in all directions at a certain wavelength.[26] Peak 2 corresponds to the emission of Trp and Tyr residues while the emission of polypeptide backbone in urease structure stands for peak 3.[28] The fluorescence intensity of peaks 2 and 3 was reduced by 35 and 74%, respectively, by addition of (*R*)-(+)-**UA** (Table S1, Supporting information). Similar spectral profile was recorded for systems containing (*S*)-(-)-**UA** (**2**) and **FPA** (**3**); reduction of fluorescence intensity of 42 and 71% was observed for peaks 2 and 3 in medium containing urease and **2** while the presence of **3** resulted in 23 and 46% decrease, respectively. The main parameters of tridimensional fluorescence are listed in Table S1.

Reduction in fluorescence intensity corresponding to peak 2 indicated changes in Tyr and Trp microenvironment while alterations related to peak 3 stand for modifications in the protein native structure. The most significant variations in fluorescence intensity were observed when the ligand was added to the medium (see peak 3 for reference), which indicates that alterations in polypeptide chain and enzyme folding took place.[37] At last, these

Published on 13 February 2018. Downloaded by Fudan University on 14/02/2018 15:52:19.
New Journal of Chemistry Accepted Manuscript

Please do not adjust margins

View Article Online
DOI: 10.1039/C8NJ00072G

Published on 13 February 2018. Downloaded by Fudan University on 14/02/2018 15:52:19.

findings are supported by the variation of Stokes shift[38] determined for native urease and respective inhibitor-enzyme complexes (Table S1).

The synchronous fluorescence is a very sensitivity technique, which provides spectral simplification and bandwidth reduction,[39] being useful for assessing changes in the urease microenvironment polarity related to Tyr and Trp residues. Stern-Volmer constant (K_{SV}) based on $\Delta\lambda$ equal to 15 nm (Tyr) and $\Delta\lambda$ equal to 60 nm (Trp) was the parameter employed to investigate urease-lichen metabolites interactions. Similar spectra profile was obtained regardless of the inhibitor added to the urease-containing system. The spectrum for urease in the presence of (*R*)-(+)-**UA** (**1**) is shown in Figure 6 to exemplify alterations in the synchronized fluorescence. Synchronous fluorescence binding parameters for lichen compounds **1-3** towards urease are shown in Table 3.

The maximum wavelength emission shift for (*R*)-(+)-**UA** (**1**) and (*S*)-(-)-**UA** (**2**) towards urease was higher for Trp than that of Tyr while no difference was detected for FPA (**3**)-containing systems (Figure 6 and Table 3). This is likely due to the fact that Tyr residues are less sensitive to the medium polarity changes when compared to Trp ones.[40] Increase in the microenvironment polarity is related to positive variation of λ_{max} while polarity reduction is associated to negative variation of λ_{max}. These phenomena allow describing changes in the structure of native protein.

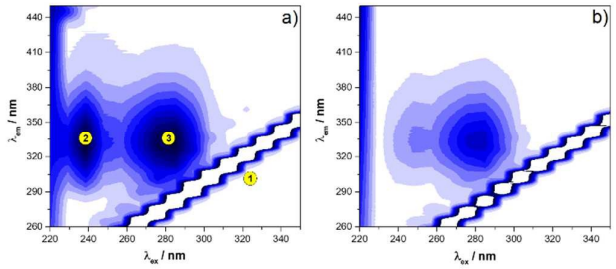

Figure 5. Tridimensional fluorescence spectra of urease (a) and (*R*)-(+)-**UA** (**1**)-urease complex (b) at pH 7.4. Enzyme and ligand were used at 1.0 and 10 μM, respectively.

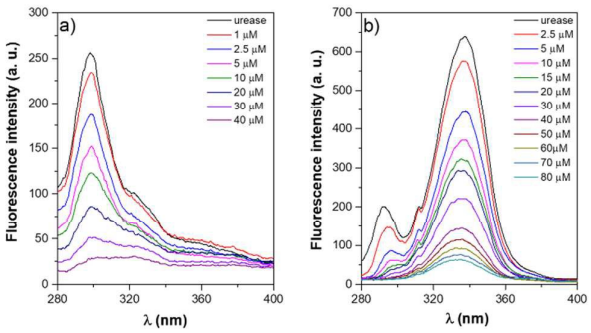

Figure 6. Urease (1.0 μM) synchronous fluorescence spectra upon addition of increasing concentrations of (*R*)-(+)-**UA** (**1**) at different concentrations in pH 7.4, monitoring (a) $\Delta\lambda$ equal to 15 nm (Tyr residues) and (b) $\Delta\lambda$ equal to 60 nm (Trp residues).

Table 3. Synchronous fluorescence binding parameters for lichen compounds **1-3** towards jack bean urease.

Lichen compound	Δλ (nm)	Stern-Volmer parameters		λ_{max} emission shift (nm)[1]
		K_{SV} (10^4 L mol^{-1})	r	
(*R*)-(+)-**UA** (**1**)	15	18.61 ± 0.18	0.9938	+1
	60	6.34 ± 0.08	0.9947	- 4
(*S*)-(-)-**UA** (**2**)	15	14.94 ± 0.22	0.9939	+ 1
	60	6.01 ± 0.11	0.9932	- 2
FPA (**3**)	15	4.81 ± 0.07	0.9923	+1
	60	4.09 ± 0.04	0.9938	+1

[1]Free urease was used as reference.

Based on K_{SV} values, Tyr residues were systematically more affected when compared to Trp ones (Table 3). We hypothesize that this is associated with the presence of Tyr at positions 410 and 544 near to key His residues (409 and 545 positions) known to coordinate to Ni atoms in the jack bean urease active site.[25,41] The Trp residues, such as those at 495 and 648 positions, are far away from urease catalytic site, suggesting that Tyr residues had their microenvironment changed more significantly than Trp ones. Notably, K_{SV} value for Tyr ($\Delta\lambda$ = 15 nm) in (*R*)-(+)-**UA** (**1**)-containing systems was higher that of urease in the presence of **1** enantiomer (compound **2**). This suggests that (*R*)-(+)-**UA** (**1**) interacts preferably with urease catalytic site in relation to its enantiomer. Indeed, kinetics results indicated that the affinity of **1** to urease active site is 3-fold higher than that of **2** (Table 1).

The influence of substrate (urea) and some classical inhibitors (thiourea, hydroxyurea and omeprazole) in the interaction of urease with lichen compounds **1-3** was evaluated by competition assay. The urease binding constant ratio (K_b'/K_b), in which K_b' and K_b refer to as the binding constant in the presence or absence of a competitor, respectively, was used for comparison purpose. Formation of urease-lichen metabolites complexes is favored when $K_b'/K_b > 1$ while ratios lower than 1 indicate that complex formation is disfavored (Table 4).

Table 4. Urease binding constants ratio in the absence (K_b) or presence (K_b') of urease substrate and inhibitors.

Lichen compound	Competitors (K_b'/K_b)			
	Substrate	Inhibitors		
	Urea	HU[1]	OMP[2]	TU[1]
(*R*)-(+)-**UA** (**1**)	0.06	0.69	0.06	0.08
(*S*)-(-)-**UA** (**2**)	0.20	0.87	0.13	0.17
FPA (**3**)	0.02	2.63	0.03	0.04

K_b' = binding constant in the presence of 25 μM substrate or inhibitor, 1.0 μM urease and lichen compounds **1-3** (1.0-80 μM). **HU**, hydroxyurea; **OMP**, omeprazole and **TU**, thiourea. Inhibitors classification: [1]competitive and [2]non-competitive.

In general, the binding constant decreases in the presence of substrate or inhibitor ($K_b'/K_b < 1$), indicating that compounds interact with urease active site. This result is in agreement with those of synchronous fluorescence (Figure 6; Table 3). All compounds tested competed with urea for urease active site. Both thiourea and hydroxyurea are competitive inhibitors.[42] Thiourea, however, was determined to be an inhibitor more effective than hydroxyurea. Besides, hydroxyurea increased **FPA** (**3**) interaction with urease. This behavior may be related to the ability of urease to catalyze hydroxyurea hydrolysis, even at a low extent.[43] Omeprazole is a urease proinhibitor (non-competitive) used for the treatment of *Helicobacter pylori*-associated diseases. It is classified as a non-competitive inhibitor by reacting with free Cys592 residue of jack bean urease, which causes blockage of urea access to the enzyme

New Journal of Chemistry Accepted Manuscript

This journal is © The Royal Society of Chemistry 20xx

Please do not adjust margins

View Article Online
DOI: 10.1039/C8NJ00072G

catalytic site.[44] The results herein presented (decreased K_b values) show that omeprazole effectively prevented lichen compounds **1-3** from binding to urease.

The (*S*)-(-)-**UA** (**2**) bound to urease and inactivated it by inducing the formation of enzyme aggregates *via* blockage of essential –SH groups.[45] It is claimed that –SH groups blockade was achieved through a nucleophilic addition into the carbonyl bond at C1 of usnic acid (Figure 1), a condition that can be reversed in the presence of Cys or dithiothreitol.[46] The mechanism of partial inactivation and reactivation of urease by (*S*)-(-)-**UA** (**2**) seems to be similar to that of omeprazole.[44b] Indeed, the kinetics and interaction profiles for (*S*)-(-)-**UA** (**2**) revealed that this lichen metabolite is a typical mixed inhibitor. Additionally, the urease enantioselectivity towards (*R*)-(+)-**UA** (**1**) may be attributed to the spatial configuration of $–CH_3$ at C9b (Figure 1) that prevents **1** from reacting with Cys592 residue and consequently being eligible to bind to the active site solely. Finally, (*R*)-(+)-**UA** (**1**) interacts preferably with urease active site by electrostatic forces as demonstrated by kinetics/interaction assays in a manner compared with other already reported for known urease inhibitors (Figure 7).

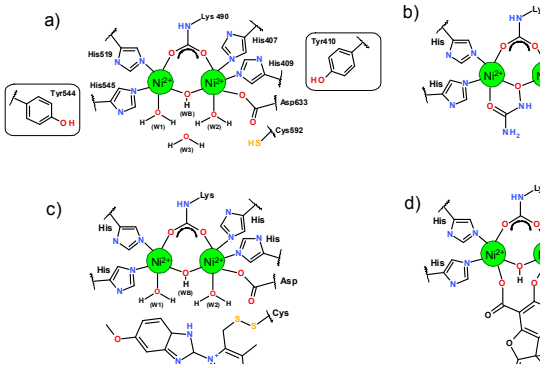

Figure 7. Schematic representation of the active site of native jack bean urease (**a**)[46] and its interaction with hydroxyurea (**b**),[47] omeprazole after reaction with Cys residue (**c**)[44a] or (*R*)-(+)-**UA** (**1**) (**d**; proposed model). W1-W3, water molecules in the active site; WB, bridging water (hydroxide form). The residues Tyr410 and Tyr544, which do not belong to urease active site were affected by the interaction process as attested by synchronous fluorescence assays.

Effect on *Helicobacter pylori* growth

The potential of lichen secondary metabolites to inhibit urease activity prompted us to investigate whether compounds **1-3** would be able to compromise *H. pylori* growth. This is because the success of *H. pylori* survival in stomach (very acidic environment) relies on its relatively high urease activity[48] and this bacterial infection is a matter of public health. The (*R*)-(+)-**UA** (**1**) was the most efficient compound against the bacterial strains tested, except for the reference strain NCTC11637 and clinical strain R40/442, whose potency was comparable to that of (*S*)-(-)-**UA** (**2**). The MIC values for compound **1** were 3.8- to 7.8-fold lower than those for omeprazole (**OMP**; reference drug) and 74- to 286-fold lower than those for hydroxyurea (**HU**) or thiourea (**TU**), known urease inhibitors (Table 5). Likewise, the other lichen natural products (**2** and **3**) were more potent than the reference drug or urease inhibitors tested. Compound **2** was 2-4-fold more efficient than **OMP**, 25-99-fold more efficient than **HU** and 39-154-fold more potent than **TU**, while the potency for compound **3** was up to 2.7-fold, 25-99-fold and 52-104-fold, respectively. Overall, the order of potency for *H. pylori* growth inhibition is **1** > **2** > **3** > **OMP** > **HU** > **TU** (Table 5). These results are in agreement with those of jack bean urease–inhibitors interaction and kinetics as well. It is noteworthy that the active site of jack bean and *H. pylori* ureases shares similarities (Figure S8, Supporting information) although the latter is constituted of two subunits while the former possesses a single amino acid chain.[41] Therefore, the allosteric site(s) targeted by (*S*)-(-)-**UA** (**2**) may be distinct from each other between the two ureases.

Published on 13 February 2018. Downloaded by Fudan University on 14/02/2018 15:52:19.
New Journal of Chemistry Accepted Manuscript

Please do not adjust margins

Published on 13 February 2018. Downloaded by Fudan University on 14/02/2018 15:52:19.

Table 5. Minimal inhibitory concentration MIC (µM and µg mL^{-1}) of lichen secondary metabolites necessary to inhibit *Helicobacter pylori* growth.

Bacterial strain*	(*R*)-(+)-UA (**1**)	(*S*)-(-)-UA (**2**)	FPA (**3**)	HU	OMP	TU
190	0.012 (4)	0.046 (16)	0.068 (32)	1.683 (128)	0.093 (32)	3.550 (256)
E17	0.012 (4)	0.023 (8)	0.034 (16)	1.683 (128)	0.093 (32)	3.550 (256)
23	0.023 (8)	0.046 (16)	0.068 (32)	3.366 (256)	0.185 (64)	3.550 (256)
110 R	0.012 (4)	0.023 (8)	0.034 (16)	3.366 (256)	0.046 (16)	0.887(64)
[1]NCTC 11637	0.023 (8)	0.023 (8)	0.068 (32)	3.366 (256)	0.093 (32)	3.550 (256)
R40/499	0.012 (4)	0.023 (8)	0.034 (16)	3.366 (256)	0.046 (16)	3.550 (256)
R40/442	0.023(8)	0.023 (8)	0.034 (16)	3.366 (256)	0.093 (32)	3.550 (256)

Hydroxyurea (**HU**), omeprazole (**OMP**) and thiourea (**TU**) were used as reference of urease inhibitors. [1]Reference strain.

*Six clinical isolates of *H. pylori* and a reference strain were tested. The MIC values were determined by broth microdilution assay in which samples were serially diluted (2-fold) in 96-well microtiter plates containing 0.1 mL of RPMI Mega Cell supplemented with 3% FCS. Values outside parentheses correspond to µM while those between parentheses refer to as the corresponding µg mL^{-1}.

New Journal of Chemistry Accepted Manuscript

View Article Online
DOI: 10.1039/C8NJ00072G

ARTICLE

Conclusions

In summary, herein it is described the isolation and structure elucidation of three secondary metabolites from the lichen *Cladonia rappii* reported for the first time at Serra do Brigadeiro State Park in Brazil. Compounds **1-3** effectively inhibited the ureolytic activity of jack bean urease with mechanisms of action typical of competitive (**1** and **3**) or mixed-inhibitor. They interact with urease by a statistic quenching mechanism with formation of non-fluorescent complexes in which the native protein structure was altered. The complexes were spontaneously formed and mainly stabilized by electrostatic forces according to the following order of strength: (*R*)-(+)-**UA** (**1**) > (*S*)-(-)-**UA** (**2**) > **FPA** (**3**). The lichen secondary metabolites were more effective than the reference drug **OMP** on inhibiting *H. pylori* growth likely due to their ability to inhibit urease. Therefore, (*R*)-(+)-**UA** (**1**) > (*S*)-(-)-**UA** (**2**) > **FPA** (**3**) may comprise excellent prototypes for further developing novel agents for the treatment of *H. pylori*-related infections.

Conflicts of interest

There are no conflicts to declare.

Acknowledgements

Authors are thankful to the Instituto Estadual de Florestas de Minas Gerais (IEF-MG/GPROP) for authorizing the harvest of *Cladonia rappii* at Serra do Brigadeiro State Park located in Araponga, Minas Gerais, Brazil, and Dr. Claudio Farina for providing two *Helicobacter pylori* clinical strains This work was supported by Fundação de Amparo à Pesquisa do Estado de Minas Gerais (FAPEMIG), Fundação de Amparo à Pesquisa do Estado de Alagoas (FAPEAL), Conselho Nacional de Desenvolvimento Científico e Tecnológico (CNPq) and Coordenação de Aperfeiçoamento de Pessoal de Nível Superior (CAPES). AF, LVM and SAF are supported by research fellowships from CNPq. We thank Camila Nunes (IQB-UFAL) for preparing Figure S8.

Experimental section

General experimental procedures

Melting points (uncorrected) were determined in a Microquímica MQRPF-301 apparatus. Optical rotation was measured on a Perkin Elmer 341 polarimeter. The IR spectrum was acquired using a Varian 660-IR gladATR spectrometer. NMR spectra were acquired on a Varian Mercury 300 MHz spectrometer using residual solvent signal as an internal standard. A high-resolution mass spectrum was acquired on a Shimadzu LCMS-IT-TOF spectrometer. The single crystal x-ray structure of compound (**2**) was determined at vaporized N_2 temperature of 150(2) K using a Bruker-AXS Kappa Apex II Duo diffractometer operating with Cu-Kα from a IμS micro-source, filtered by multi-layer mirror x-ray optics. Structure solution was obtained using Direct Methods implemented in SHELXS and the final refinement was performed with full matrix least squares on F2 using SHELXL. The softwares ORTEP-3[49] and SHELXS/SHELXL[50] were used from WinGX[51] package. Column chromatography was performed on silica gel 60 (53-200 μM). Fractions were monitored by TLC, and spots were visualized by heating plates with a solution of acid vaniline. Vacuum liquid chromatography[52] was performed using a 2 L sintered funnel and silica gel 60 (53-200 μM).

Lichen material

Cladonia rappii A Evans was harvested in July (2012) at Serra do Brigadeiro State Park located in Araponga, Minas Gerais, Brazil (20°41'26.85''S, 42°28'20.41''W, 1644 m). The lichen species was identified by Dr. Suzana M. A. Martins from the Natural Sciences Museum of Rio Grande do Sul (Pelotas, RS, Brazil) and deposited in the herbarium of the Department of Botany at the Federal University of Viçosa (MG, Brazil) under the voucher specimen number VIC 35,603. The *Cladonia rappii* harvesting for this study was authorized by the Brazilian National Council for Scientific and Technological Development (CNPq; process # 010026/2014-2).

Isolation of secondary metabolites from the lichen

Powdered and dried lichen (84.7 g) was extracted with acetone (600 mL) at room temperature for seven days. The acetone extract was filtered and evaporated under reduced pressure to afford the crude extract (12.46 g), which was resuspended in hot acetone:ethanol 20:1 and maintained overnight at -10°C to yield a yellow precipitate referred to as the crude usnic acid (**UA**). Recrystallization with acetone/ethanol 95% (5:1) afforded yellow needles of compound **2** (3.60 g, 4.2%). After that, the remainder crude extract was evaporated under reduced pressure, resuspended in hot acetone:chloroform 20:1 and kept at -10 °C for 24 h to furnish a grey precipitate determined to be a crude fumarprotocetraric acid (**FPA**; **3**). The suspension was filtered and the precipitate was washed with

Published on 13 February 2018. Downloaded by Fudan University on 14/02/2018 15:52:19.

New Journal of Chemistry Accepted Manuscript

Please do not adjust margins

View Article Online
DOI: 10.1039/C8NJ00072G

Published on 13 February 2018. Downloaded by Fudan University on 14/02/2018 15:52:19.

chloroform (3x10 mL) and acetone (3x20 mL) to afford **3** (2.33 g, 2.75%) as a pure pale grey powder. The (*R*)-(+)-**UA** (**1**) was purchased from Sigma-Aldrich.

Derivatization of fumarprotocetraric acid [FPA (3)]

One drop of triethylamine was added directly into an NMR tube containing a solution of **FPA** (**3**; 6 mg / 600 µL, DMSO-d_6). After 10 min, the NMR tube was shaked for recording the ^{1}H NMR spectrum of triethylamine salt obtained.[21]

(*S*)-(-)-Usnic acid [(*S*)-(-)-UA (2)]

Yellow, needle-shaped crystals; Mp 193.7-194.3 °C; $[\alpha]_{20}^{d}$ = -391.0 (c 0.7, $CHCl_3$); IR (neat) ν_{max} 1627, 1605, 1283 e 1067 cm^{-1}; ^{1}H NMR (300 MHz, $CDCl_3$) δ 18.84 (1H, s, OH-3), 13.30 (1H, s, OH-7), 11.02 (1H, s, OH-9), 5.97 (1H, s, H-4), 2.66 (3H, s, 6-$OCCH_3$), 2.65 (3H, s, 2-$OCCH_3$), 2.08 (1H, s, H-8), 1.75 (1H, s, H-9b); ^{13}C NMR (75 MHz, $CDCl_3$) δ 201.7 (2-$OCCH_3$), 200.3 (6-$OCCH_3$), 198.0 (C-1), 191.6 (C-3), 179.3 (C-4a), 163.8 (C-7), 157.4 (C-9), 155.1 (C-6a), 109.2 (C-8), 105.2 (C-2), 103.9 (C-9a), 101.4 (C-6), 98.3 (C4), 59.0 (C-9b), 32.1 (C-9b), 31.3 (6-$OCCH_3$), 27.9 (2-$OCCH_3$), 7.5 (C-8); HRESITOFMS *m/z* 343.0792 [M-H]- (Calculated for $C_{18}H_{15}O_7$, *m/z* 343.0817). Figures S2 and S3 presented the ^{1}H and ^{13}C NMR spectra, respectively (Supporting information).

Fumarprotocetraric acid [FPA (3)]

Pale, grey and amorphous powder; IR (neat) ν_{max} 3094, 1747, 1699, 1655, 1615, 1575, 1155 cm^{-1}. ^{1}H NMR (300 MHz, DMSO-d_6) δ 11.97 (1H, s, H-7' or H-4'' or OH-2' or OH-4), 10.57 (1H, s, H-9), 6.84 (1H, s, H-5), 6.64 (2H, s, H-2'', H-3''), 5.30 (2H, s, H-9'), 2.45 (3H, s, H-8), 2.42 (3H, s, H-8'); ^{13}C NMR (75 MHz, DMSO-d_6) δ 191.6 (C-9), 170.1 (C-7'), 165.2 (C-4''), 164.6 (C-1''), 163.9 (C-2), 163.9 (C-4), 160.9 (C-7), 155.3 (C-2'), 152.0 (C-6), 145.4 (C-4'), 142.1 (C-5'), 135.0 (C-3''), 132.2 (C-2''), 131.9 (C-6'), 116.8 (C-5), 117.2 (C-1′), 113.3 (C-3'), 112.1 (C-3), 112.0 (C-1), 56.8 (C-9'), 21.3 (C-8), 14.6 (C-8'). HRESITOFMS *m/z* 471.0603 [M-H]$^-$ (Calculated for $C_{22}H_{15}O_{12}$, *m/z* 471.0566). Figures S4 and S5 presented the ^{1}H and ^{13}C NMR spectra, respectively (Supporting information).

Fumarprotocetraric acid triethylamine salt (3a)

^{1}H NMR (300 MHz, DMSO-d_6) δ 10.40 (1H, s, H-9), 6.63 (1H, d, *J* = 15.6 Hz, H-3''), 6.24 (1H, d, *J* = 15.6 Hz, H-2''), 6.08 (1H, s, H-5), 5.14 (2H, s, H-9'), 2.52 (1H, s, H-8'), 2.48 (1H, s, H-8). Figure S6 presented the ^{1}H NMR spectrum (Supporting information).

Urease activity assay

The potential of compounds **1-3** to inhibit the activity of jack bean type III urease was investigated essentially as described elsewhere[53] using hydroxyurea as reference of inhibitor and all compound-test at 1 mM. Buffered reactions (pH 7.0) containing increasing concentration of urea (1 to 32 mM), 12.5 mU jack bean type II urease and each inhibitor (individually) at fixed concentrations (0.2, 0.4 or 0.8 mM) were performed to assess the mechanism by which compounds **1**–**3** inhibit the ureolytic activity of urease. Jack bean urease kinetic parameters such as initial velocity (V_o), K_M (Michaelian constant) and maximum velocity (V_{max}) were obtained using Hyper32 software (hyper32.sharewarejunction.com). The double reciprocal plots were obtained using the OriginPro8 (Origin Lab, Northamptom, MA) software. The α and the α' values were used to calculate the equilibrium dissociation constants for urease-inhibitor complex (K_i) and for urease-urea-inhibitor complex (K'_i).[23]

Interaction studies by molecular fluorescence

Stock solutions of *Canavalia ensiformis* (jack bean) type III urease (Sigma-Aldrich) at 10 µM was prepared in 20 mM phosphate buffer (pH 7.4) while the lichen compounds **1-3** were dissolved in DMSO to yield 1.0 mM solutions that were further diluted in phosphate buffer to provide the corresponding working solutions. Molecular fluorescence titrations were performed using quartz cuvettes of 10 mm optical path on a Shimadzu spectrofluorimeter (model 5301PC, Japan) equipped with xenon lamp (150 W). The urease (1.0 µM) fluorescence emission spectra in the absence or presence of lichen compounds **1-3** (1 to 80 µM) were recorded from 250 to 450 nm employing λ_{ex} of 280 nm at three temperatures (23, 30, 38 ºC). The excitation and emission slits were 5 and 10 nm, respectively. Tridimensional fluorescence experiments were performed using excitation wavelength in the range from 220-350 nm and fixed emission range from 260 to 450 nm. Synchronous fluorescence spectra for urease in the absence or presence of lichen compounds **1-3** were obtained by simultaneous variation of excitation and emission monochromators. The difference in the excitation wavelength (Δλ) was fixed individually at Δλ equal to 15 nm and Δλ equal to 60 nm to show solely spectroscopic behavior of Tyr and Trp residues, respectively. As for the competitive assay, urease substrate (urea) and inhibitors (**HU**, **OMP** or **TU**) were used at the fixed concentration of 25 µM in the competitive assay.

Bacterial strains culture

Six clinical isolates of *H. pylori,* and a reference strain of *H. pylori* (ATCC 43504) were included for this study. The strains were maintained at -80 °C in Wilkins Chalgren Broth (Difco, BD, San Jose, CA, USA) with 10% (v/v) horse serum (Seromed, Biocrhom, Germany) and 20% (v/v) glycerol (Merck, Darmstadt, Germany). The strains were subcultured on Columbia agar base (Difco, BD, San Jose, CA, USA) supplemented with 10% horse serum and 0.25% bacto yeast extract (Difco, BD, San Jose, CA, USA). Plates were incubated for 72 h at 37 °C in an atmosphere of 10% CO_2 in a gas incubator.

Determination of minimum inhibitory concentration (MIC)

The MIC values were determined by modified broth dilution method as previously described.[54] Briefly, two-fold serial dilution of compounds-test were prepared in a 96-well microtiter plate

New Journal of Chemistry Accepted Manuscript

This journal is © The Royal Society of Chemistry 20xx

View Article Online
DOI: 10.1039/C8NJ00072G

containing 100 µL of MegaCellTM RPMI-1640 medium (Sigma-Aldrich, ST Louis, MO, USA) supplemented with 3% fetal calf serum (FCS). An inoculum equivalent to 1 McFarland standard was prepared in Wilkins Chalgren broth and diluted in MegaCell^{TM} RPMI-1640 medium containing 3% FCS. Each well was inoculated with *H. pylori* at a final concentration of approximately 5×10^5 CFU. Plates were incubated at 37 °C under microaerophilic conditions (10% CO_2 in a gas incubator) and examined after 72 h of incubation.

Supporting information

This material is available free of charge via the Internet at http://pubs.acs.org." Information: Figures: The reaction for formation triethylamine salt of fumarprotocetraric acid, ^1H and ^{13}C NMR spectra of lichen compounds **2** and **3**, Van't Hoff plot for interaction between lichen compounds and urease at different temperatures. Table: Tridimensional fluorescence parameters for free urease by itself or in the presence of lichen compounds **1-3**.

Notes and references

1 T. H. Nash, *Lichen Biology*; Cambridge University Press: New York, 2008.

2 J. Boustie, S. Tomasi and M. Grube, *Phytochem. Rev.,* 2011, **10**, 287.

3 F. H. Curd and A. Robertson, *J. Chem. Soc.* 1933, 1173.

4 Ingólfsdóttir, K. *Phytochemistry,* 2002, **61**, 729.

5 (*a*) K. Ingólfsdóttir, G. A. Chung, V. G. Skúlason, S. R. Gissurarson and M. Vihelmsdóttir, *Eur. J. Pharm. Sci.,* 1998, **6**, 141; (*b*) I. Francolini, P. Norris, A. Piozzi, G. Donelli and P. Stoodley, *Antimicrob. Agents Chemoter.,* 2004, **48**, 4360; (*c*) N. K. Honda, F. R. Pavan, R. G. Coelho, S. R. de Andrade Leite, A. C. Micheletti, T. I. Lopes, M. Y. Misutsu, A. Beatriz, R. L. Brum and C. Q. Leite, *Phytomedicine,* 2010, **17**, 328; (*d*) S. Kim, R. Greenleaf, M. C. Miller, L. Satish, S. Kathju, G. Ehrlich, J. C. Post, N. G. Sotereanois and O. Stoodley, *J. Mater. Sci.: Mater. Med.,* 2011, **22**, 2773; (*e*) V. K. Gupta, S. Verma, S. Gupta, A. Singh, A. Pal, S. K. Srivastava, P. K. Srivastava, S. C. Singh and M. P. Darokar, *Eur. J. Clin. Microbiol. Infect. Dis.,* 2012, **31**, 3375; (*f*) R. H. Pires, R. Lucarini and M. J. Mendes-Giannini, *Antimicrob. Agents Chemother.,* 2012, **56**, 595.

6 (*a*) K. C. S. Kumar and K. Müller, *J. Nat. Prod.,* 1999a, **62**, 817; (*b*) K. C. S. Kumar and K. Müller, *J. Nat. Prod.* 1999b, **62**, 821; (*c*) G. A. de Paz, J. Raggio, M. P. Gómez-Serranillos, O. M. Palomino, E. González-Burgos, M. E. Carretero and A. Crespo, *J. Pharm. Biomed. Anal.,* 2010, **53**, 165.

7 (*a*) L. Campanella, M. Delfini, P. Ercole, A. Iacoangeli and G. Risuleo, *Biochimie,* 2002, **84**, 329; (*b*) D. N. Sokolov, V. V. Zarubaev, A. A. Shtro, M. P. Polovinka, O. A. Luzina, N. I. Komarova, N. F. Salakhutdinov and O. I. Kiselev, *Bioorg. Med. Chem. Lett.,* 2012, **22**, 7060.

8 (*a*) C. Bézivin, S. Tomasi, I. Rouaud, J. G. Delcros and J. Boustie, *Planta Med.,* 2004, **70**, 874; (*b*) M. A. Bazin, A. C. Le Lamer, J. G. Delcros, I. Rouaud, P. Uriac, J. Boustie, J. C. Corbel and S. Tomasi, *Bioorg. Med. Chem.,* 2008, **16**, 6860.

9 C. S. Vijayakumar, S. Viswanathan, M. K. Reddy, S. Parvathavarthini, A. B. Kundu and E. Sukumar, *Fitoterapia,* 2000, **71**, 564.

10 M. Bruno, B. Trucchi, B. Burlando, E. Ranzato, S. Martinotti, E. K. Akkol, I. Süntar, H. Keles and L. Verotta, *Bioorg. Med. Chem.,* 2013, **21**, 1834.

11 Y. Asahina and Y. Tanase, *Ber. Dtsch. Chem. Ges.,* 1934, **67**, 411.

12 N. Neamati, H. Hong, A. Mazumder, S. Wang, S. Sunder, M. C. Nicklaus, G. W. A. Milne, B. Proksa and Y. Pommier, *J. Med. Chem.,* 1997, **40**, 942.

13 G. M. B. Alves, M. B. S. Maia, E. S. Franco, A. M. Galvão, T. G. da Silva, R. M. Gomes, M. B. Martins, E. P. S. Falcão, C. M. M. B. de Castro and N. H. da Silva, *Pulm. Pharmacol. Ther.,* 2014, **27**, 139.

14 R. C. Tigre, N. H. Silva, M. G. Santos, N. K. Honda, E. P. S. Falcão and E. C. Pereira, *Ecotoxicol. Environ. Saf.,* 2012, **84**, 125.

15 X. Y. Jiang, L. Q. Sheng, C. F. Song, N. N. Du, H. J. Xu, Z. D. Liu and S. S. Chen, *New J. Chem.,* 2016, **40**, 3520.

16 (*a*) D. T. Smoot, H. L. T. Mobley, G. R. Chippendale, J. F. Lewison and J. H. Resau, *Infect. Immun*., 1990, **58**, 1992; (*b*) J. K. Xu, C. S. Goodwin, M. Cooper and M. Robinson, *J. Infect. Dis.,* 1990, **161**, 1302.

17 J. G. Romagni, G. Meazza, N. P. D. Nanayakkara and F. E. Dayan, *Febs Lett.,* 2000, **480**, 301.

18 H. G. M. Edwards, E. M. Newton and D. D. Wynn-Williams, *J. Mol. Struct.,* 2003, **651-653**, 27.

19 M. A. Rashid, M. A. Majid and M. A. Quader, *Fitoterapia,* 1999, **70**, 113.

20 S. Parsons, H. D. Flack and T. Wagner, *Acta Crystallogr.,* 2013, **B69**, 249.

21 B. N. Su, M. Cuendet, D. Nikolic, H. Kristinsson, K. Ingólfsdóttir, R. B. van Breemen, H. H. S. Fong, J. M. Pezzuto and A. D. Kinghorn, *Magn. Reson. Chem.,* 2003, **41**, 391.

22 L. P. Horta, Y. C. C. Mota, G. M. Barbosa, T. C. Braga, I. E. Marriel, A. de Fátima and L. V. Modolo, *J. Braz. Chem. Soc.,* 2016, **27**, 1512.

23 D. Voet and J. Voet, J. *Biochemistry*. John Wiley & Sons: New York, 2011

24 J. Zhang, X. J. Wang, Y. J. Yan and W. S. Xiang, *J. Agric. Food Chem*., 2011, **59**, 7506.

25 K. Takishima, T. Suga and G. Mamiya, *Eur. J. Biochem*., 1988, **175**, 151.

26 W. Y. Qing and Z. Hong-Mei, *Spectrochim. Acta, Part A,* 2012, **96**, 352.

27 J. R. Albani, Principles and applications of fluorescence spectroscopy; Wiley-Blackwell: Oxord, 2007

28 M. D. A. Dantas, H. A. Tenório, T. I. B. Lopes, H. J. V. Pereira, A. J. Marsaioli, I. M. Figueiredo and J. C. C. Santos, *Int. J. Biol. Macromol.,* 2017, **102**, 505.

29 C. M. da Silva, M. M. Silva, F. S. Reis, A. L. T. G. Ruiz, de J. E. Carvalho, J. C. C. Santos, I. M. Figueiredo, R. B. Alves,

Published on 13 February 2018. Downloaded by Fudan University on 14/02/2018 15:52:19.

New Journal of Chemistry Accepted Manuscript

Please do not adjust margins

View Article Online
DOI: 10.1039/C8NJ00072G

L. V. Modolo and A. de Fátima, *J. Photochem. Photobiol. B,* 2017, **172**, 129.
30 X. Li, D. Chen, G. Wang and Y. Lu, *Eur. J. Med. Chem.,* 2013, **70**, 22.
31 H. M. Zhang, G. C. Zhang and Y. Q. Wang, *Biol. Trace Elem. Res.,* 2011, **141**, 53.
32 Y. Q. Wang, G. C. Zhang and H. M. Zhang, *J. Solution Chem.,* 2011, **40**, 458.
33 K. Yamasaki, V. T. G. Chuang, T. Maruyama and M. Otagiri, *Biochim. Biophys. Acta,* 2013, **1830**, 5435.
34 P. Zhang, D. Liu, Z. Li, Z. Shen, P. Wang, M. Zhou, Z. Zhou and W. Zhu, *J. Lumin.,* 2014, **155**, 231.
35 T. Sarwar, M. A. Husain, S. U. Rehman, H. M. Ishqia and M. Tabish, *Mol. BioSyst.,* 2015, **11**, 522.
36 P. H. Ross and S. Subramanian, *Biochemistry,* 1981, **20**, 3096.
37 Q. Wang, X. Liu, M. Su, Z. Shi and H. Sun, *Spectrochim. Acta, Part A,* 2015, **136**, 320.
38 H. Zhang, Y. Zou and E. Liu, *Spectrochim. Acta, Part A,* 2012, **92**, 283.
39 S. Bobone, M. van de Weert and L. Stell, *J. Mol. Struct.,* 2014, **1077**, 68.
40 F. Sun, W. Zong, R. Liu, J. Chai and Y. Liu, *Spectrochim. Acta, Part A,* 2010, **76**, 142.
41 A. Balasubramanian and K. Ponnuraj, *J. Mol. Biol.,* 2010, **400**, 274.
42 F. M. Oliveira, L. C. A. Barbosa, A. J. Demuner, C. R. A. Maltha, S. R. Pereira, L. P. Horta and L. V. Modolo, *Med. Chem. Res.,* 2014, **23**, 5174.
43 J. F. Marlier, L. I. Robins, K. A. Tucker, J. Rawlings, M. A. Anderson and W. W. Cleland, *Biochemistry,* 2010, **49**, 8213.
44 (*a*) Z. Amtul, A. Rahman, R. A. Siddiqui and M. I. Choudhary, *Curr. Med. Chem.* 2002, **9**, 1323; (*b*) T. C. Kuehler, J. Fryklund, N. Bergman, J. Weilitz, A. Lee and H. Larsson, *J. Med. Chem.,* 1995, **38**, 4906.
45 (*a*) C. Vicente and B. Cifuentes, *Plant Sci. Lett.,* 1979, **15**, 165. (*b*) A. Gonulez and B. Cifuentes, *Phytochemistry,* 1986, **25**, 1063.
46 B. Krajewska and M. Brindell, *J. Therm. Anal. Calorim.,* 2016, **123**, 2427.
47 B. Krajewska and W. Zaborska, *Bioorg. Chem.,* 2007, **35**, 355.
48 J. M. Maroney and S. Ciurli, *Chem. Rev.* 2014, **114**, 4206.
49 L. J. Farrugia, *J. Appl. Crystallogr.,* 1997, **30**, 565.
50 G. M. Sheldrick, *Acta Crystallogr.,* 2008, **64**, 112.
51 L. J. Farrugia, *J. Appl. Crystallogr.,* 1999, **32**, 837.
52 J. C. Coll and B. F. Bowden, *J. Nat. Prod.,* 1986, **49**, 934.
53 (*a*) T. O. Brito, A. X. de Souza, Y. C. C. Mota, V. S. S. Morais, L. T. de Souza, A. de Fátima, F. C. Macedo-Júnior and L. V. Modolo, *RSC Adv.,* 2015, **5**, 44507; (*b*) D. P.de Araujo, V. S. S. Morais, A. de Fátima and L. V. Modolo, *RSC Adv.,* 2015, **5**, 28814.
54 F. Sisto, M. M. Scaltrito, G. Russello, A. Bonomi and F. Dubini, *Curr. Microbiol.,* 2009, **58**, 559.

Published on 13 February 2018. Downloaded by Fudan University on 14/02/2018 15:52:19.
New Journal of Chemistry Accepted Manuscript

This journal is © The Royal Society of Chemistry 20xx

View Article Online
DOI: 10.1039/C8NJ00072G

In vitro inhibition of *Helicobacter pylori* and interaction studies of lichen natural products with jack bean urease

Tiago C. A. Lage, Thamilla Maria S. Maciel, Yane C. C. Mota, Francesca Sisto, José R. Sabino, Josué C. C. Santos, Isis M. Figueiredo, Carla Masia, Ângelo de Fátima, Sergio A. Fernandes, Luzia V. Modolo

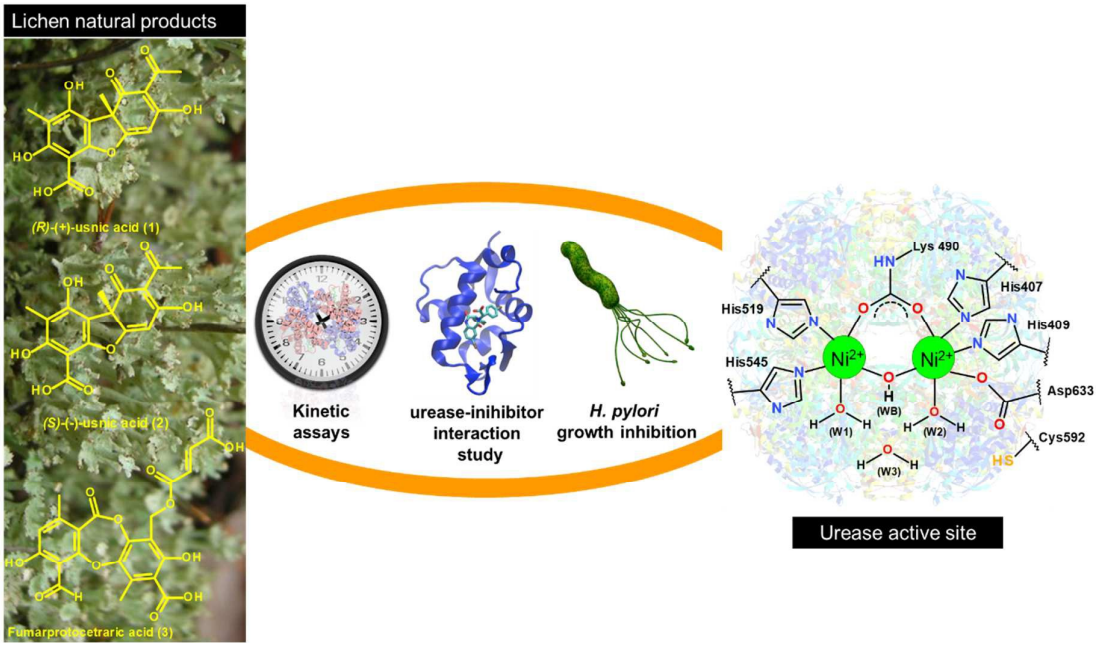

Published on 13 February 2018. Downloaded by Fudan University on 14/02/2018 15:52:19.

New Journal of Chemistry Accepted Manuscript